A short climatological study of cold air pools and drainage flows in small valleys

Bradley Jemmett-Smith[1], Andrew N Ross[1], Peter Sheridan[2]
[1] School of Earth and Environment, University of Leeds, Leeds, LS2 9JT, UK
[2] Met Office, Exeter, EX1 3PB, UK
Corresponding author: Andrew N Ross <A.N.Ross@leeds.ac.uk>

Abstract

This paper uses detailed observations from the COLd air Pooling EXperiment (COLPEX) to study the frequency and characteristics of cold air pooling in a small-scale valley typical of much of the southern UK and other lowland regions of the world. The field experiment took place in and around the Clun Valley, Shropshire, England during July 2009-April 2010, which was a particularly cold winter with a record low in the NAO index. Cold pools, defined here as where the minimum valley temperature overnight is at least 1°C colder than the surrounding hill tops, occur on 45% of nights over the observational period, with strong cold pools (>4°C temperature difference) occurring on 12% of nights. As might be expected, cold pool formation is closely linked to conditions with clear skies and light winds, often associated with high pressure situations. Cold pools are also closely linked with weak down valley drainage flows. This contrasts with non-cold pool nights or daytime conditions where several other mechanisms also contribute to the observed winds in the valley. The data set highlights the importance of cold air pools and drainage flows, even in quite moderate terrain, and the impact this can have on local microclimates.

Introduction

Cold air pools form (usually at night) in valleys when radiative cooling leads to the formation of cold air near the surface which drains down and collects in the valley bottom. The process is well known and can be important for night-time minimum temperatures, with impacts on road icing, fog formation and air quality. The relatively small size of a typical UK valley means that these cold pools are not observed by the operational surface network as the average spacing between Met Office sites is ~40 km and are not usually captured even in the Met Office 1.5km UKV operational model.

The COLd air Pooling EXperiment (COLPEX; Price et al, 2011) was an extensive field experiment designed to observe cold air pools in small UK scale valleys. The experiment ran from July 2009 – April 2010 around the Clun Valley, Shropshire, UK. The Clun Valley has a width of 1-2 km and depth of ~100-150m and is representative of many small valleys in the UK and other lowland, temperate and mid-latitude regions of the world. A number of cases from COLPEX have already been studied in detail and compared with high resolution (100m) numerical simulations (Vosper et al 2014; Hughes et al 2015). This case study approach has also been used in a number of other recent studies in other parts of the world although they often look at larger scale valleys (e.g. Lareau et al, 2013) or enclosed basins (Whiteman et al, 2008). Hawke (1944) took long term observations from 1929 to the mid 1940s in the Rickmansworth valley in Hertfordshire, characterising the frost hollow in the valley. Galvin (2005a,2005b) revisited the Rickmansworth valley and identified the change in the valley climate, as a result of increased urbanisation since the 1940s. The study of Pepin et al (2009) is notable in focussing on a smaller scale valley in Finland, although the high latitude leads to distinctive features due to the extreme length of the days in summer and nights in winter. Other UK case studies of small frost hollows (as opposed to valleys) include Graham (2012) and Burt (1997). This paper will look at the COLPEX dataset from a climatological standpoint to see what the frequency and characteristics of cold pools are in a small valley such as the Clun Valley.

The Clun Valley and COLPEX field experiment

The Clun Valley, is situated in a rural location near the Welsh-English border. The land is largely pasture land for grazing sheep and cattle, with some arable farming on the lower parts of the valley. There are also small patches of woodland dotted along the valley. The underlying geology is Silurian sandstone, mudstone and siltstone, giving rise to rounded hills, with quite steep valley sides. The rock is overlaid with free-draining acid brown soil over higher ground, with richer silts and glacial clay on the valley floors.

The COLPEX experiment took place from July 2009 – April 2010 and involved extensive measurements in and around the Clun Valley including 3 measurement towers observing wind speed, temperature, humidity and turbulent flux measurements at several heights up to 30m or 50m above the ground. These were complemented by a network of 22 HOBO temperature and humidity loggers and 10 automatic weather stations (AWS, which measured winds and pressure in addition to air temperature and humidity). Here we focus primarily on the towers at Duffryn (on the valley floor) and at Springhill (hilltop to the south of the valley), and on HOBO and AWS data in the valley. Figure 1 shows the Clun Valley and the location of the sites. Figure 2 shows a selection of photographs of the Clun valley, illustrating the rolling hills and the mixture of pasture land with small wooded areas. The photos also illustrate the 50m mast at Duffryn and one of the AWS sites. Price *et al* (2011) give a fuller description of the experimental setup.

The winter of 2009-10 was unusually cold, the coldest since 1978/9, with mean UK temperatures 2.0°C below the 1971-2000 average (Prior and Kendon, 2011) and rainfall just 77% of the average, with the west of the UK being the driest relative to normal. The weather patterns were dominated by winds with a northerly or easterly component (Prior and Kendon, 2011). These conditions explain the relatively dry winter on the west side of the country. However several periods of low pressure led to precipitation and occasional periods of snow cover, particularly from mid December through to mid January. Over the winter, the Welsh borders saw 20-30 days of snow cover. These unusual conditions were linked with record low values of the NAO index for December – March (Osborn, 2011). The data set is too short to strictly be considered a climatology, in particular since the period concerned is not necessarily representative of the longer term climatology of the region. Nonetheless it provides a rare detailed set of measurements of cold pool characteristics over a number of months.

Cold pool characteristics

Here, cold pool strength is measured using a pair of HOBO temperature and humidity data loggers, one sited on the valley floor (HOBO 2, 200m above mean sea level) and the second on the adjacent hilltop (HOBO 16, 360m above mean sea level). Data were available from 23rd July 2009 to 16 April 2010. For each night the cold pool strength is defined as the maximum 10-minute average temperature difference between the hilltop and valley sites over the course of the night. A night is defined as a cold air pool night in this instance if this value is greater than 1°C. Nights where the cold pool strength was greater than 4°C were classified as strong cold pools. Figure 3a shows the distribution of cold pool strengths across the whole field campaign, while Figure 3b gives a breakdown of cold pool strength by month. What is clear from these figures is the ubiquity of cold pools in this valley during the study period, with 56% of nights having a maximum cold pool strength greater than 1°C, and 20% of nights exceeding 4°C. The cold pools were distributed throughout the year, although there was a slight bias to stronger cold pools over the winter

months (likely caused by longer nights, by weaker morning convection delaying CAP break-up and in some cases by snow cover). The two strongest cold pools (9.0°C and 9.6°C) are clear outliers and occurred in January when there was very cold weather and snow lying on the ground. On these nights temperatures reached -17.9°C and -18.2°C respectively. Even putting these two aside, there were 15 nights when the cold pool strength exceeded 6°C. This is substantial given that there is only 160m height difference between the two HOBO sites. Although not shown, similar distributions of cold pools were observed with other pairs of valley floor / hill top measurements along the Clun Valley.

Figure 3c shows the time at which the maximum cold pool strength occurred for all cold pool and strong cold pool events. Cold pool strength can peak at any time during the night, though there is an increase in occurrence later in the night and around dawn. In particular, almost all of the strong cold pool events have their maximum later in the night, with a clear peak in the hour following sunrise. The spread of maximum strength throughout the night is likely a reflection of the frequency with which conditions can change during the night leading to the weakening or removal of the cold pool. The strongest cold pools occur on nights where the cold pool can continue to develop throughout the night, and so in these cases the maximum strength is most likely to be observed around sunrise. The fact that for a large number of cases the maximum occurs after sunrise is likely due to a combination of the fact that valleys are shaded and so there may be a delay after sunrise before direct sun reaches the valley floor and that erosion of the stable boundary layer by heating at the surface does not occur immediately at sunrise.

This definition of cold pool strength based on two measurements provides no information on the depth of the cold pool, and could possibly mask cases where there is a shallow cold pool with an adiabatic layer above. Figure 4 shows the temperature difference across upper and lower layers of the valley on cold pool nights using a third HOBO part way up the valley side (HOBO 18, 310m above mean sea level). In almost all cases the temperature gradient in the bottom half of the valley was higher than in the top half (points to the right of the green line). For all cold pool cases the temperature increased with height over the bottom half of the valley, while the temperature in the top half could be either increasing or decreasing with height. In a number of cases the gradient in the upper half of the valley was actually close to or larger than the dry adiabatic lapse rate (points below the red dashed line) suggesting a shallow cold pool in the lower half of the valley with an adiabatic layer above, while in other cases the upper part of the valley was as stable as the lower part of the valley, suggesting a deep cold pool. Interestingly, some of the very strongest cold pools (orange +), were almost exclusively confined to the bottom half of the valley, with temperature differences close to zero over the upper part of the valley. While the measurements here do not allow a precise evaluation of the cold pool depth, they do suggest a variety of cold pool depths depending on the conditions. Although not shown, temperature gradients between 1.2m and 25m and between 25m and 50m on the tower at Duffryn were also investigated . These were much more scattered, but showed air temperature increasing with height at both levels for all cold pool cases, suggesting the cold pools were usually deeper than 50m. These conclusions are consistent with the radiosonde profiles of temperature observed at Duffryn for a number of IOPs (intensive observation periods) during COLPEX.

The strong cooling in cold pools is sometimes associated with the formation of valley fog. Fog formation only occurred in a small proportion of cold pool cases during COLPEX. Visibility and rainfall was measured in the valley at Duffryn using a Biral HSSVPF-730 present weather sensor. Over the 9 months of the field campaign there were 24 days (92 hours in total) on which visibility was below 1km (aviation fog) and only 9 days (15 hours) when visibility was less than 180 m (thick

fog). As a percentage, these correspond to 8.0% and 3.3% of days, respectively. There were no occurrences of dense fog with visibility less than 50m. Unlike the cold pool strength, there is a strong seasonal variation in the occurrence of fog, with the vast majority of cases occurring during December – February (81 out of the 92 hours). In terms of timing, fog can occur throughout the day, although the most common times are overnight, particularly towards dawn, when the cold pools are strongest. Again, the unusual conditions of winter 2009/10 may not make this a representative estimate of the climatological occurrence of fog. Ongoing work on fog formation in such small-scale valleys forms part of the Local And Non-local Fog EXperiment (LANFEX; Price et al, 2018).

Controls on cold pool formation

Figure 5 shows the distribution of cold pools as a function of the mean night-time wind speed and direction outside the valley, and F_{lw} (the ratio of the mean night time downwelling to upwelling long wave radiation). For clear sky nights with little cloud cover the downwelling longwave radiation is much less than the upwelling radiation (small F_{lw}), leading to radiative cooling, while for cloudy nights downwelling and upwelling longwave radiation are similar and so F_{lw} is close to 1. The wind speed and direction are measured at 30m AGL (above ground level) at the Springhill site on the hill top adjacent to the Clun Valley. Long wave radiation components are measured at 2m AGL at the Duffryn site on the valley floor. As might be expected, cold pool nights (particularly strong cold pool nights) favour low wind conditions, although even with very low wind speeds there are still nights on which a cold pool is not formed. There is also a close link between wind direction and cold pool formation. It is likely that much of this is due to the correlation in the data between wind direction and other factors: prevailing SW winds tend to be stronger and are often associated with potentially cloudy low pressure systems, while high pressure systems with slack winds and clearer skies are often linked with more northerly or easterly winds. There is however also the possibility that the wind direction can directly promote or suppress cold pool formation and drainage flows either through channelling of the wind down or up the valley, or through the large scale pressure gradient aiding or opposing the drainage flow. Northerly winds for example not only tend to be associated with high pressure systems and light winds, but also lead to a west-east, i.e. down valley pressure gradient. These effects are hard to disentangle with the available observations and additional measurements in valleys with different orientations are really needed to understand this fully.

As might be expected, cold pool formation is also strongly linked to clear skies, quantified through F_{lw}. Nights without cold pools typically have high values of F_{lw}. (>0.93 more than 65% of the time), while cold pool nights have values of F_{lw} less than 0.93 at least 80% of the time, and there are no cases of strong cold pools with a value of F_{lw} larger than this. Wind speed, coupled with cloud cover, therefore provide the best indicators for cold pooling conditions. This agrees well with a more quantitative study of cold pool formation in COLPEX by Sheridan et al (2014) and with the idealised numerical study of Vosper and Brown (2008).

Drainage flows in the valley

Wind measurements were made at multiple heights at the 3 main sites, and also at a single height (2m) at a number of automatic weather stations distributed around the Clun valley and its tributary valleys (see Figure 1). Figure 6 shows wind roses at 2m and 50m from the Duffryn site in the Clun valley. The wind roses are based on 10-minute mean winds over the whole night. Results are shown for all nights, and just for cold pool nights. In all cases night time wind speeds are low

(<5 ms^{-1} at 2m) reflecting the sheltered nature of the valley. Wind directions are predominantly down valley, although for some non-cold pool nights up valley or across valley flow is observed, but this is relatively uncommon. Wind speeds are higher at 50m, and slightly more westerly in direction, particularly on cold pool nights. This likely reflects the cases where the cold pool is less than 50m deep and so the wind direction at 50m is less strongly coupled to the near surface winds. Figure 6 also shows wind speeds at 2m in one of the side valleys. AWS 7 is in a N-S aligned side valley (see Figure 1) to the north of the Clun valley, northeast of Duffryn. The side valley is steeper and narrower than the main Clun valley. Compared to the measurements at Duffryn, the flow in the side valley is even more constrained along the valley axis, and mostly from the north. In cold pool conditions the flow is almost exclusively down valley, while for some other nights there is up-valley flow.

Figure 7 reinforces this interpretation by showing the probability distribution of hourly averaged winds as a function of both the ambient wind direction (at Springhill, 30m above ground level, AGL) and the wind direction at Duffryn (2m or 50m AGL). This approach was taken by Whiteman and Doran (1993) to study the mechanisms driving flow in a larger valley. For nights with stronger ambient winds at Springhill (>5 ms^{-1}) and for daytime conditions the hilltop and valley winds are strongly coupled (most points lie along the solid black line), while for lighter ambient winds (<5 ms^{-1} at Springhill) the flow within the valley is predominantly along-valley (NW winds in the valley irrespective of the wind direction at hill top, blue dashed line). The decoupling is strongest at Duffryn (2m), with a greater likelihood of the 50m wind direction aligning with the Springhill ambient hill top wind direction if the cold pool is less than 50m deep. Even at 2m AGL and for wind speeds less than 5ms^{-1} there are some occasions when the valley flow is coupled to the flow aloft. This happens primarily when the flow at the hill top has a strong up valley component, which can overcome a weak drainage flow and prevent formation of a cold pool. The other two mechanisms proposed by Whiteman and Doran (1993) are channelled flow, either forced-channelling (black dash-dot line) or pressure driven channelling (green dotted line). At Duffryn there is little evidence of either of these mechanisms.

Figure 7 also shows probability distributions of winds at AWS 7, where there is predominantly N (down-valley) flow on low wind speed nights. The steeper and narrower valley at AWS 7 leads to a more constrained flow direction than in the Clun valley, even during the day. The primary difference is that for windy nights or during the day southerly winds are much more likely when there is a southerly component to the ambient wind, compared to low wind speed nights. The requirement for a southerly wind component and the fact these similar up valley winds occur both on windy nights and during the day suggests that these are largely channelled flow rather than thermally driven up-valley winds. Comparing the data to the black dash-dot line (forced channelling) and the green dotted line (pressure driven channelling) suggests that pressure driven channelling may play a role in this side valley, unlike in the main Clun valley.

The threshold of 5 ms^{-1} for low wind night-time conditions is consistent with those used in previous studies, however choosing a different (but still low) threshold leads to qualitatively similar results and so the general conclusions are not too sensitive to this choice. Taking a more stringent condition and only plotting results for strong cold pool nights (not shown) gives even stronger dominance of down-valley flow.

Conclusions

Cold air pooling and drainage flows are well acknowledged processes, but there is a lack of data available with which to quantify their strength and frequency. This detailed data set gives an insight into cold air pool statistics in a typical lowland English valley. Perhaps the most striking aspect of the data is the frequency with which cold pools form and the large temperature differences that can occur, even in small valleys. Although observers often report such cold air pooling events, and locals often know about individual frost pockets, the wider public often forget how import such small-scale processes are in determining night time minimum temperatures. Winter 2009/10 was particularly cold in the UK, which may well have increased the frequency and strength of the cold pools, however they were observed to occur frequently through the year and not just during the particularly cold winter. Wind speed, coupled with cloud cover, provide the best indicators for cold pooling conditions. Wind measurements show that overnight wind flow in these small valleys is dominated by down-valley drainage flows, particularly on low wind speed nights conducive to cold air pooling. Whether the daytime valley flow is coupled to the ambient flow, or channelled down the valley seems dependent on the valley size and geometry. Together all these features clearly illustrate the significant impact of cold pools on the local climate in a valley. The lower night-time temperatures would lead to a significantly increased risk of road icing and impact crop growth. Downscaling forecast data using the ideas developed from the COLPEX project offers a useful way to provide more detailed road temperature forecasts for local authorities and highway authorities (Sheridan et al, 2010; Sheridan, Vosper and Smith, 2018).

References

Burt S. (1997) The Altnaharra minimum temperature of -27.2°C on 30 December 1995. *Weather* **52** 134-144. doi: 10.1002/j.1477-8696.1997.tb06294.x
Galvin J.F.P. (2005a) The effects of urbanisation in the Rickmansworth valley: part 1 – observations. *Weather* **60** 115-120. doi: 10.1256/wea.53.04
Galvin J.F.P. (2005b) The effects of urbanisation in the Rickmansworth valley: part 2 – probable causes of the modified valley climate. *Weather* **60** 150-152. doi: 10.1256/wea.54.04
Graham, E. (2012) A Hebridean frost hollow made visible. *Weather* **67** 45-47. doi: 10.1002/wea.809
Hawke E.L. (1944) Thermal characteristics of a Hertfordshire frost-hollow. *Q. J. R. Meteorol. Soc.* **70** 23-48. doi: 10.1002/qj.49707030306
Hughes J.K., Ross A.N., Vosper S.B., Lock A., Jemmett-Smith B.C. (2015) Assessment of valley cold pools and clouds in a very high resolution NWP model. *Geosci. Model Dev.* **8** 3105-3117. doi: **10.5194/gmd-8-3105-2015**
Laureau N.P., Crosman E., Whiteman C.D., Horel J.D., Hoch S.W., Brown W.O.J., Horst T.W. (2013) The Persistent Cold-Air Pool Study. *Bull. Am. Meteorol. Soc.* 94, 51-63. doi: 10.1175/BAMS-D-11-00255.1
Osborn T.J. (2011) Winter 2009/10 temperatures and a record-breaking North Atlantic Oscillation index. *Weather* **66** 19-21. doi: 10.1002/wea.660

Pepin N.C., Schaefer M.K., Riddy L.D. (2009) Quantification of the cold air pool in Kevo valley Finnish Lapland. *Weather* **64** 60-67. doi: 10.1002/wea.260

Price J.D., Vosper S., Brown A., Ross A.N., Clark P., Davies F., Horlacher V., Claxton B., McGregor J. R., Hoare J.S. (2011) COLPEX: Field and Numerical Studies Over a Region of Small Hills. *Bull. Am. Meteorol. Soc.* **92**, 1636-1650. doi: 10.1175/2011BAMS3032.1

Price J.D., Lane S., Boutle I.A., Smith D.K.E., Bergot T., Lac C., Duconge L., McGregor J., Kerr-Munslow A., Pickering M., Clark R. (2018) LANFEX: a field and modeling study to improve our understanding and forecasting of radiation fog . *Bull. Am. Meteorol. Soc.* Early online release. doi: 10.1175/BAMS-D-16-0299.1

Prior J. and Kendon M. (2011) The UK winter of 2009/10 compared with severe winters of the last 100 years. *Weather* **66** 4-10. doi: 10.1002/wea.735

Sheridan P.F., Smith S.A., Brown A.R., Vosper S.B. (2010) A simple height-based correction for temperature downscaling in complex terrain. *Meteorol. Appl.* **17,** 329–339. doi: 10.1002/met.177

Sheridan P.F., Vosper S.B., Brown A.R. (2014) Characteristics of cold pools observed in narrow valleys and dependence on external conditions. *Q. J. R. Meteorol. Soc.* **140** 715-728. doi: 10.1002/qj.2159

Sheridan P.F., Vosper S.B., Smith S.A. (2018) A physically-based algorithm for downscaling temperature in complex terrain. *J. Appl. Meteol. Climatol.* Accepted.

Vosper S.B., Brown A.R. (2008) Numerical simulations of sheltering in valleys: The formation of nighttime cold-air pools. *Boundary-Layer Meteorol.* **127** 429-448. doi: 10.1007/s10546-008-9272-3

Vosper S.B., Hughes J.K., Lock A.P., Sheridan P.F., Ross A.N., Jemmett-Smith B., Brown A.R. (2014) Cold pool formation in a narrow valley. *Q. J. R. Meteorol. Soc.* **140**. 699-714. doi: 10.1002/qj.2160

Whiteman C.D., Doran J.C. (1993) The relationship between overlying synoptic scale flows and winds within a valley. *J. Appl. Meteorol.* **32** 1669-1682. doi: 10.1175/1520-0450(1993)032<1669:TRBOSS>2.0.CO;2

Whiteman C.D., Hoch S.W., Hahenberger M., Muschinski A., Hohreiter V., Behn M., Cheon Y., Zhong S., Yao W., Fritts D., Clements C.B., Horst T.W., Brown W.O.J., Oncley S.P. (2008) METCRAX 2006: Meteorological Experiments in Arizona's Meteor Crater, *Bull. Am. Meteorol. Soc.* **89**, 1665-1680. doi: 10.1175/2008BAMS2574.1
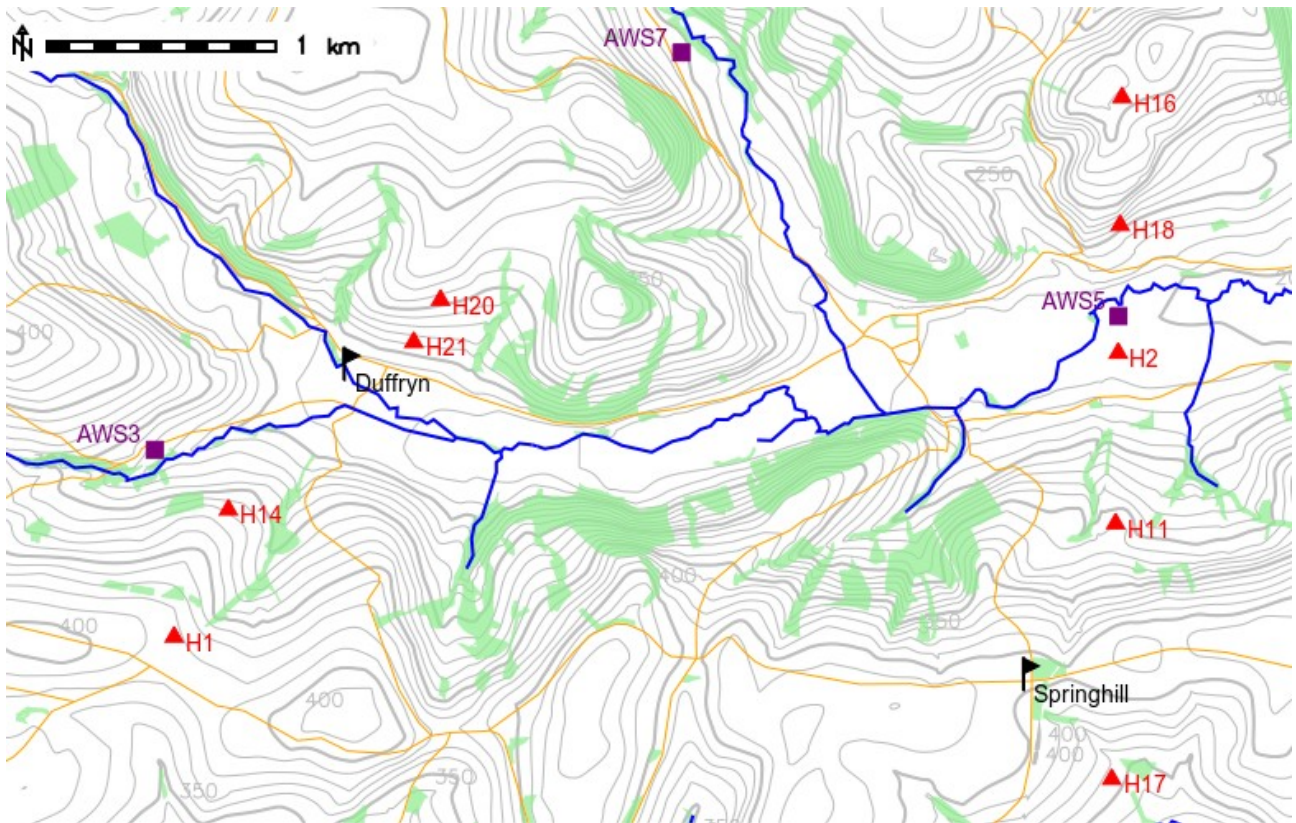
Figure 1: Map showing the central part of the Clun Valley. Marked are the main measurement sites (black flags), AWS (green squares) and HOBO loggers (red triangles). Height contours are plotted at intervals of 10m, with thicker, labelled, contours every 50m. Map data is © Crown Copyright and Database Right 2018. Ordnance Survey (Digimap Licence)

Figure 2: Selection of photos showing views of the Clun valley. The photo on the right shows the 50m mast at Duffryn and the bottom middle photo shows one of the valley floor AWS. Photos are taken by Andrew Ross (top left, top middle) and Bradley Jemmett-Smith (top right, bottom left, bottom middle).
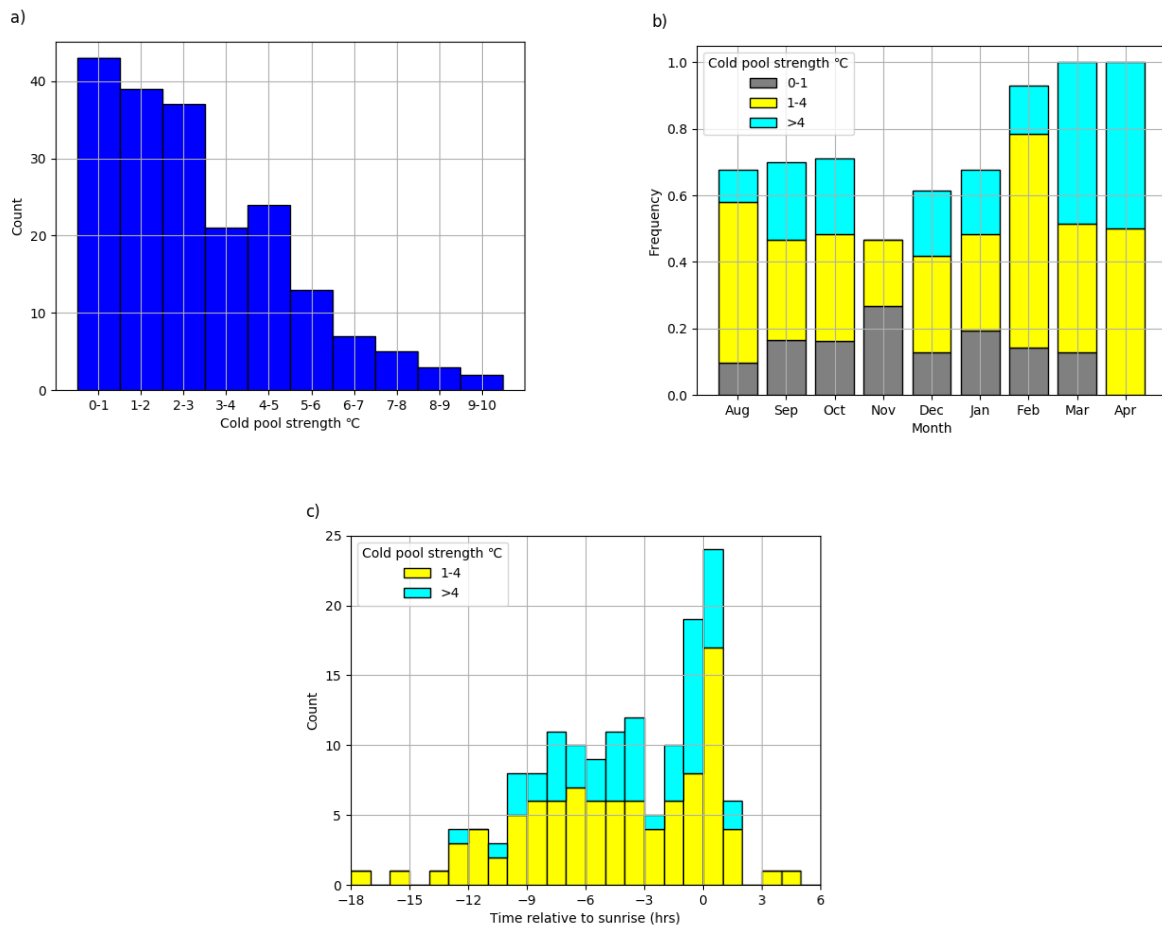
Figure 3: Cold air pooling occurrence (a) number of events as a function of cold pool strength, (b) frequency of events (categorised by cold pool strength) for each month 1st August 2009 – 16th April 2010 and (c) number of events (cold pool or strong cold pool) as a function of time of maximum cold pool strength relative to sunrise.
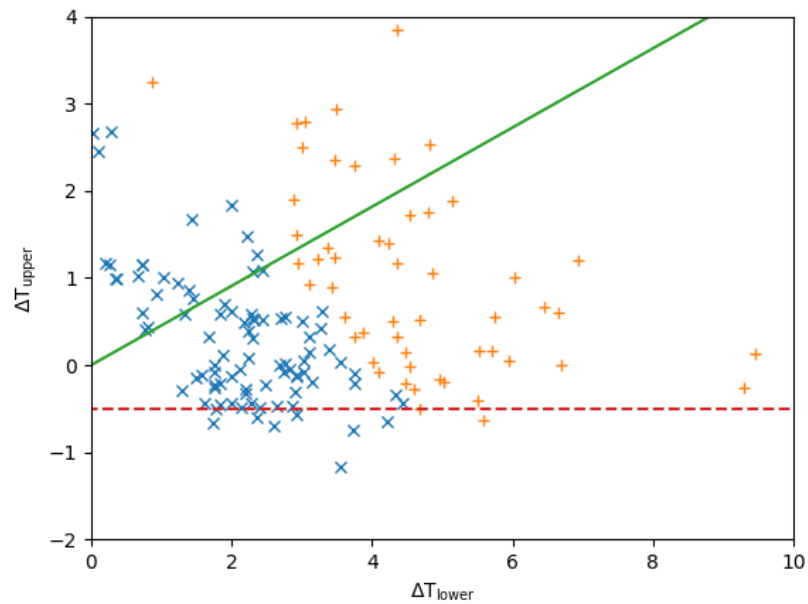
Figure 4: Temperature difference over an upper layer of the valley (HOBO 16 – HOBO 18) against temperature difference over a lower layer of the valley (HOBO 18 – HOBO 2) at the time of maximum cold pool strength for cold pool nights. Blue x mark are for cold pools with strength <4°C and orange + are for strong cold pools with strength >4°C. The solid green line is for constant temperature gradient over lower and upper parts of the valley. The red dashed line is for a dry adiabatic cooling rate of 10°C / km in the upper layer of the valley.
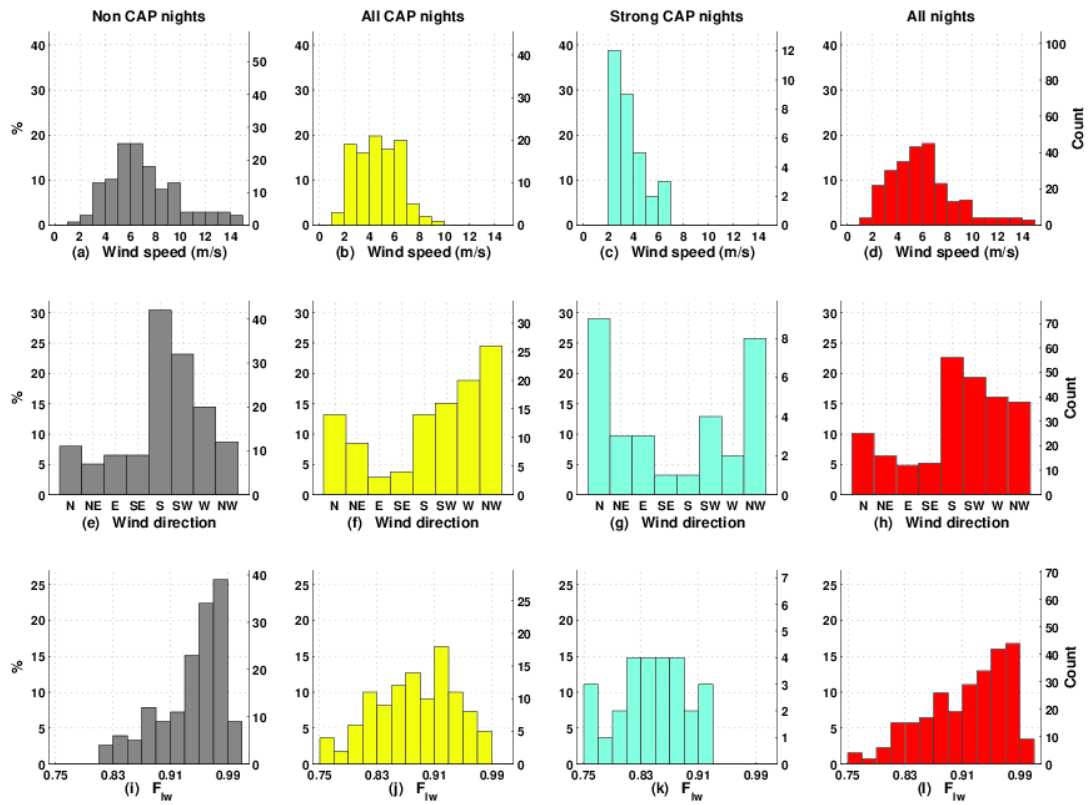
Figure 5: Frequency distribution of nights as a function of wind speed, wind direction (both at 30m above ground level at the hilltop Springhill site) and ratio of downwelling to upwelling long wave radiation (F_{lw}) (measured in the valley at Duffryn) for non-cold pool nights, all cold pool nights, strong cold pool nights and all nights.
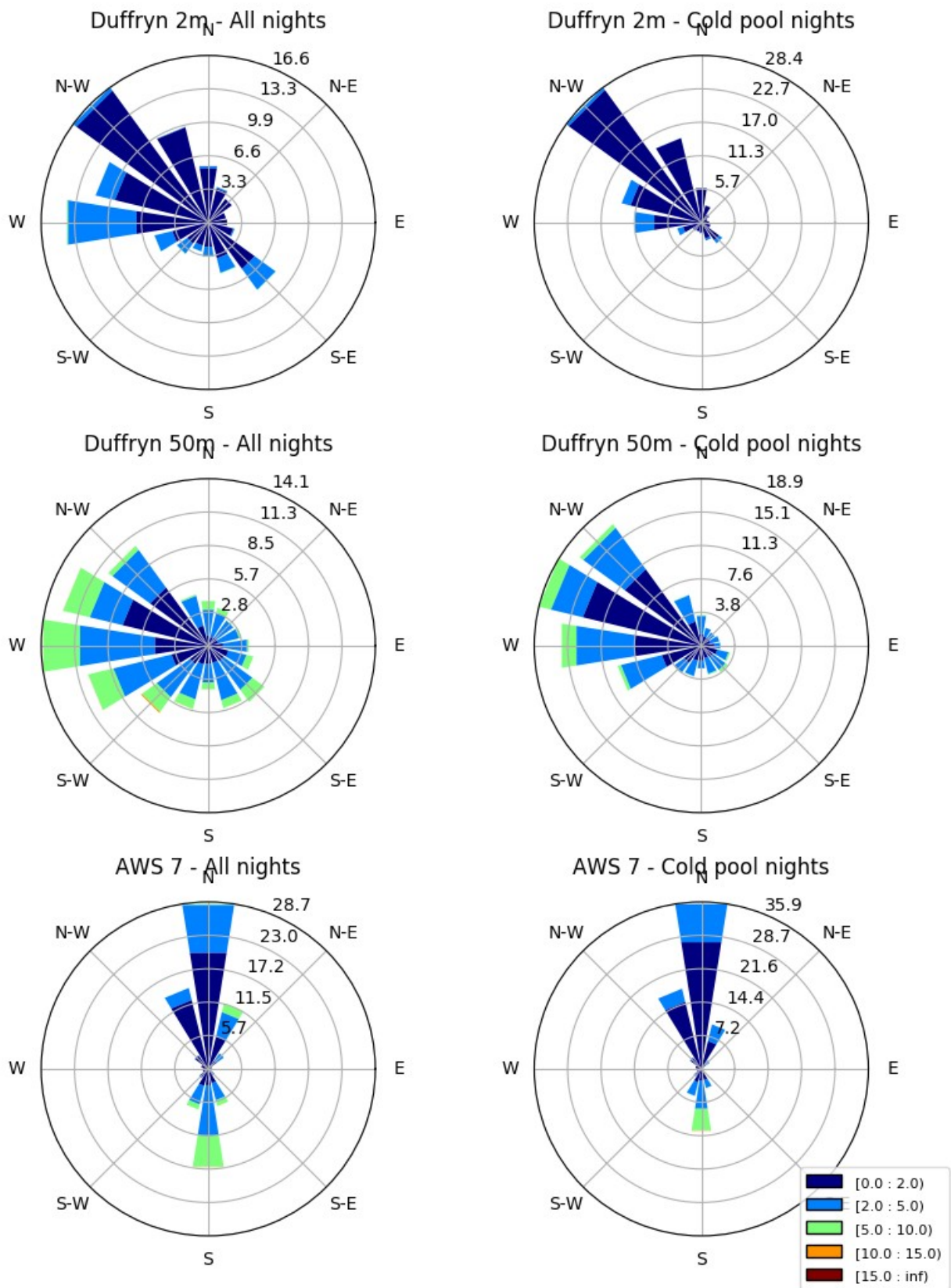
Figure 6: Wind rose plots of 2m (top) and 50m (middle) wind speed at Duffryn and 2m wind speeds at AWS 7 (bottom) for all nights (left) and cold pool nights only (right)
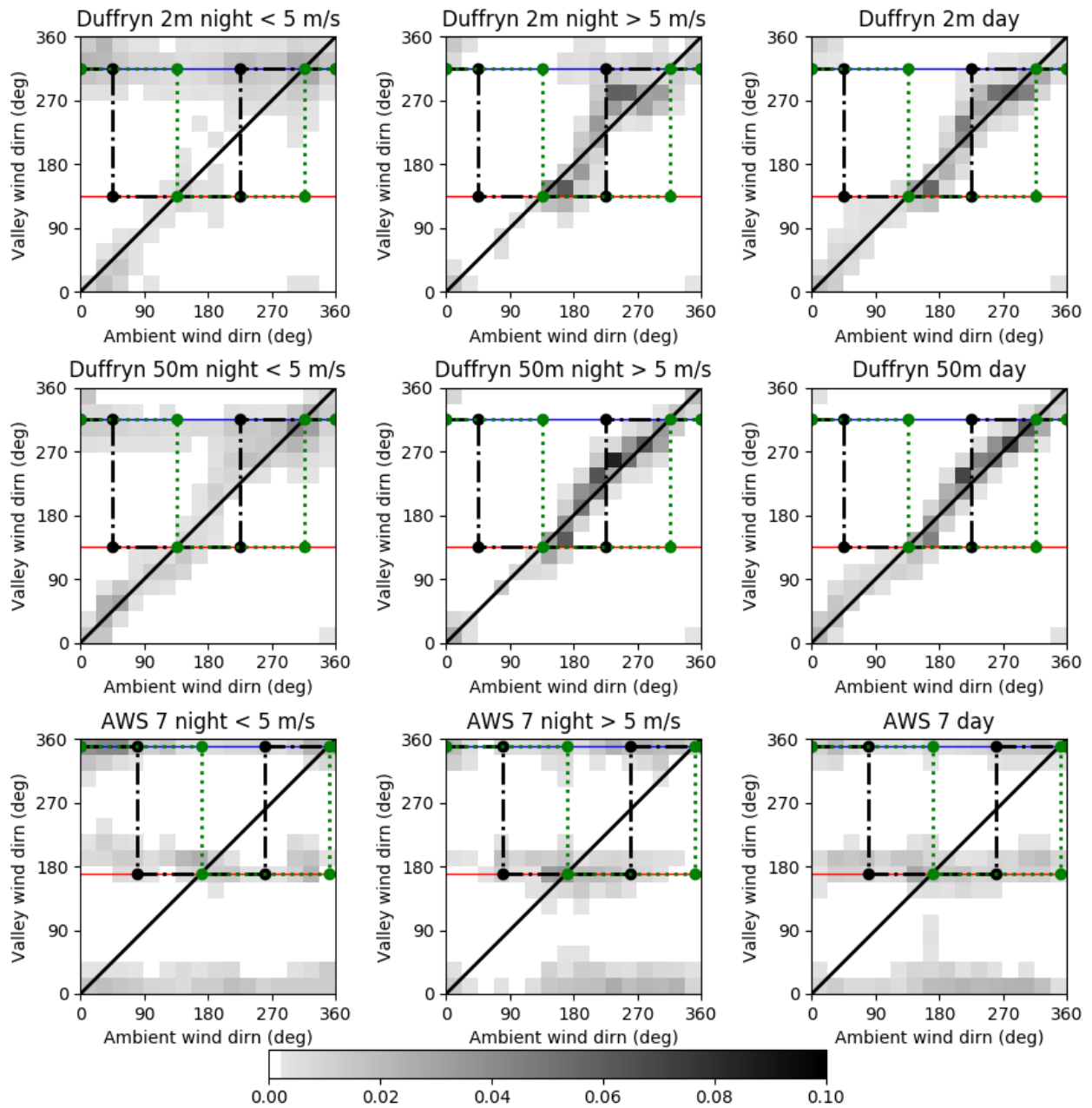
Figure 7: Probability distribution of 1 hour averaged wind directions as function of the valley wind at Duffryn (2m or 50m AGL) and AWS 7 versus the ambient wind at Springhill (30m AGL) for low ambient wind speed (<5ms^{-1}) and high ambient wind speed (>5ms^{-1}) nights and for daytime. The solid black line shows coupled flow, solid blue line shows down-valley flow, the solid red line shows up-valley flow, the black dashed-dotted line shows wind channelled flow and the green dotted line shows pressure driven flow. Wind direction observations are sorted into 16 bins of 22.5° width.